Microenvironment and Immunology

Cancer Research

Complementary Actions of Inhibitors of Angiopoietin-2 and VEGF on Tumor Angiogenesis and Growth

Hiroya Hashizume[1], Beverly L. Falcón[1], Takashi Kuroda[1], Peter Baluk[1], Angela Coxon[2], Dongyin Yu[2], James V. Bready[2], Jonathan D. Oliner[2], and Donald M. McDonald[1]

Abstract

Inhibition of angiopoietin-2 (Ang2) can slow tumor growth, but the underlying mechanism is not fully understood. Because Ang2 is expressed in growing blood vessels and promotes angiogenesis driven by vascular endothelial growth factor (VEGF), we asked whether the antitumor effect of Ang2 inhibition results from reduced sprouting angiogenesis and whether the effect is augmented by inhibition of VEGF from tumor cells. Using Colo205 human colon carcinomas in nude mice as a model, we found that selective inhibition of Ang2 by the peptide-Fc fusion protein L1-7(N) reduced the number of vascular sprouts by 46% and tumor growth by 62% over 26 days. Strikingly, when the Ang2 inhibitor was combined with a function-blocking anti-VEGF antibody, the number of sprouts was reduced by 82%, tumor vascularity was reduced by 67%, and tumor growth slowed by 91% compared with controls. The reduction in tumor growth was accompanied by decreased cell proliferation and increased apoptosis. We conclude that inhibition of Ang2 slows tumor growth by limiting the expansion of the tumor vasculature by sprouting angiogenesis, in a manner that is complemented by concurrent inhibition of VEGF and leads to reduced proliferation and increased apoptosis of tumor cells. *Cancer Res; 70(6); 2213–23. ©2010 AACR.*

Introduction

Inhibitors of vascular endothelial growth factor (VEGF) that are widely used in cancer therapy reduce angiogenesis (1), cause regression of tumor vessels, slow tumor growth (2, 3), and may improve drug delivery (4, 5). VEGF inhibitors have documented antitumor effects (6–8), but drug resistance eventually occurs, and other strategies for affecting the tumor vasculature are being sought (9). Inhibitors of angiopoietins are among the promising antiangiogenic approaches under development (10–13).

Angiopoietins are Tie2 receptor ligands that play key roles in vascular development, angiogenesis, and remodeling. Angiopoietin-1 (Ang1) tends to stabilize blood vessels and promote vascular maturation (14). Ang2 is expressed in growing blood vessels (15, 16) and promotes angiogenesis and tumor growth (17, 18) by destabilizing blood vessels (16, 19, 20). Vascular destabilization may involve Ang2 acting as an inhibitor or partial agonist of Tie2, which opposes the stabilizing action of Ang1 on endothelial cells (21, 22).

Inhibition of Ang2 may promote vessel stability and reduce angiogenesis (10). Because Ang2 promotes the proangiogenic action of VEGF (16, 19, 20), and VEGF upregulates Ang2 expression in endothelial cells (23), inhibition of Ang2 and VEGF together could have complementary actions by reducing sprouting angiogenesis and tumor vascularity (19, 24, 25).

Multiple approaches have been used to inhibit Ang2 to explore effects on angiogenesis and tumor growth. Among these are genetic deletion of host-derived Ang2 (26), neutralization of angiopoietins by soluble Tie2 receptors that function as decoys (27, 28), selective Ang2-binding aptamers (29, 30), and antibodies and peptibodies (peptide-Fc fusion proteins) that selectively neutralize the action of Ang2 (13, 25).

The goals of the present study were to gain a better understanding of the mechanisms that underlie the slowing of tumor growth by Ang2 inhibitors and determine whether these actions can add to the effects of inhibiting VEGF. First, we sought to learn whether inhibition of Ang2 reduces the blood supply of tumors by decreasing endothelial cell sprouting, increasing tumor vessel regression, or both. Second, we determined whether the slowing of tumor growth results from reduced tumor cell proliferation, increased tumor cell death, or both. Finally, we asked whether the effects of Ang2 inhibitors complement the effects of concurrent inhibition of VEGF on tumor vessels and tumor cells.

Toward this end, we used an Ang2-binding peptibody called L1-7(N) to block the action of Ang2 in human Colo205 colon carcinoma cells implanted in nude mice (13, 31). The

Authors' Affiliations: [1]Cardiovascular Research Institute, Comprehensive Cancer Center, and Department of Anatomy, University of California, San Francisco, California and [2]Oncology Research, Amgen, Inc., Thousand Oaks, California

Note: Supplementary data for this article are available at Cancer Research Online (http://cancerres.aacrjournals.org/).

H. Hashizume and B.L. Falcón contributed equally to this work.

Corresponding Author: Donald M. McDonald, Department of Anatomy, S1363, University of California, 513 Parnassus Avenue, San Francisco, CA 94143-0452. Phone: 415-476-2118; Fax: 415-502-0418; E-mail: donald.mcdonald@ucsf.edu.

doi: 10.1158/0008-5472.CAN-09-1977

Ang2 inhibitor was administered alone or in combination with an anti-human VEGF antibody that neutralized the action of tumor cell–derived VEGF. The Colo205 tumor model was used because of its documented sensitivity to Ang2 inhibitors (13).

Materials and Methods

Tumor model and treatment. CD1 *nu/nu* mice with implanted human Colo205 colon xenografts were treated with the Ang2-selective peptibody L1-7(N) (13) and/or monoclonal anti-human VEGF antibody with a median neutralization dose of 0.04 to 0.08 μg/mL against rat and human VEGF (clone 26503; R&D Systems). L1-7(N) has an IC_{50} of 71 pmol/L against murine Ang2 and comparable inhibitory activity against human Ang2 (13) but does not bind Ang1, Ang3, Ang4 (13), or angiopoietin-like proteins 3 and 4.[3] As negative controls, tumor-bearing mice were also treated with human Fc (hFc) or mouse IgG2. Agents were administered twice per week for 26 d. The total L1-7(N) dose of 700 μg/mouse/week administered s.c. exceeds the optimal biological dose of L1-7(N) in the Colo205 tumor model (13). The optimal anti-VEGF antibody dose of 200 μg/mouse/week i.p. was based on pilot experiments (data not shown). No weight loss was found in mice receiving any of the treatments.

The treatment groups were (*a*) hFc and normal IgG2, (*b*) L1-7(N), (*c*) anti-VEGF antibody, and (*d*) L1-7(N) and anti-VEGF antibody together. Control protein or isotype control antibody was added to the treatment groups to match the total amount of protein delivered in the combination group. Tumor length, width, and height were measured with calipers, and the volume was calculated using the formula for volume of an ellipsoid. All experimental procedures were conducted in accordance with institutional guidelines established by the Institutional Animal Care and Use Committees at the University of California, San Francisco and Amgen, Inc.

PCR measurements of gene expression. Expression of murine and human Ang2, Tie2, VEGF, and VEGFR-2/KDR was measured by Taqman real-time PCR (RT-PCR) using species-specific probe sets (Supplementary Table). DNase-treated total RNA (100 ng per reaction) was extracted from Colo205 tumors and 22 other human tumor xenografts implanted s.c. in immunocompromised mice (four to five mice per tumor type). *In vitro* transcribed mRNA for each gene of interest was used as the standard for calculating absolute copy numbers. Taqman RT-PCR was performed with the Taqman EZ RT-PCR kit (Applied Biosystems).

Immunohistochemistry, staining, and microscopy. Mice were perfused with fixative and tumors were processed and stained as previously described (3). Viable regions of tumor were marked by YO-PRO-1 (1:1,000; Invitrogen/Molecular Probes), which is a fluorescent dye that stains intact nuclei (32). Necrotic regions of tumors did not stain with YO-PRO-1. Endothelial cells were identified by hamster anti-CD31 antibody (clone 2H8, 1:500; Thermo Scientific). Basement membrane was marked with rabbit anti–type IV collagen antibody (1:20,000; CosmoBio). Proliferating cells were identified with rabbit anti–phosphohistone-H3 (1:1,000; Millipore/Upstate Biotechnology), and apoptotic cells were marked with rabbit anti-activated caspase-3 (1:1,000; R&D Systems). Secondary antibodies were goat anti-hamster or anti-rabbit IgG labeled with FITC or Cy3 (1:400; Jackson ImmunoResearch). Tumors were stained with H&E for conventional light microscopy. Specimens were examined with a Zeiss Axiophot fluorescence microscope or a Zeiss LSM510 confocal microscope as previously described (31).

Image measurements. Sections were cut roughly through the central of each tumor and stained with YO-PRO-1 to distinguish viable regions (YO-PRO-1 positive) from necrotic regions (YO-PRO-1 negative). Multiple low-magnification (2.5× objective) digital images, each measuring 5.1 × 3.8 mm, were used to create a montage of composite images in Adobe Photoshop. After adjusting the green fluorescence threshold, typically 25 to 30 (range, 0–255), the total number of YO-PRO-1–positive pixels was determined with ImageJ software (33). The area of viable tumor was calculated as the number of YO-PRO-1–positive pixels, each having an area of 64 μm^2.

Area density and total area of blood vessels (CD31), proliferating cells (phosphohistone-H3), and apoptotic cells (activated caspase-3) were measured in five digital images (1280 × 960 μm in size; 10× objective lens). Four of the images were taken in each quadrant of the tumor perimeter and one in the center of an 80-μm-thick section. Fractional area (area density) of CD31, phosphohistone-H3, or activated caspase-3 immunoreactivity was measured as the number of pixels above the fluorescence threshold (typically 15–30) within YO-PRO-1–positive regions (3, 34). The total area of CD31, phosphohistone-H3, or activated caspase-3 immunoreactivity was calculated as the product of the fractional area and the total area of YO-PRO-1–positive pixels. Values for total area of immunoreactivity were thus influenced by tumor size, but those for area density were not.

Endothelial cell sprouts were counted in real-time fluorescence microscopic images of tumor vessels of sections 60 μm in thickness stained for CD31 (10× objective; 2× Optovar) as previously described (31, 35). The area density of platelet-derived growth factor receptor-β (PDGFR-β)–positive pericytes within 10 μm of tumor vessels was measured on confocal microscopic images as previously described (31).

Statistical analysis. Values are expressed as the mean ± SE for four to five mice per group. Tumor growth curves reflect seven mice per group. Effect of treatment on tumor growth was calculated as the difference between the volume increase of experimental tumors and the volume increase of control tumors expressed as a percentage of the control tumor volume increase. The significance of differences was determined by ANOVA followed by the Fisher's pairwise least significant difference or Dunn-Bonferroni post hoc test. Differences in tumor growth curves were tested

[3] A. Saiki et al., unpublished data.

by repeated-measures ANOVA and Scheffé's post hoc test. P values of <0.05 were considered statistically significant.

Results

Angiopoietin and VEGF expression in Colo205 and other tumor xenografts. Taqman RT-PCR measurements revealed that untreated human Colo205 xenografts in nude mice expressed abundant human and mouse Ang2 and VEGF (Table 1). Expression of human Ang2 and human and mouse VEGF in Colo205 tumors was near the median value of 23 different xenograft models, and expression of mouse Ang2 was the highest (Table 1). Human VEGF in Colo205 tumors had 5-fold the expression of mouse VEGF and 17-fold the expression of human Ang2. Expression of human and mouse Tie2 in all tumor types and of human VEGFR-2/KDR in some tumor types was below the threshold of detection (<1,000 copies).

Treatment-related slowing of tumor growth. Tumors in mice treated with hFc increased >3-fold in volume from an average of 277 mm^3 on day 1 to 871 mm^3 on day 23 of treatment (Fig. 1A, i). Tumors grew more slowly in the other groups. Compared with the hFc group, the increase in tumor volume was reduced 62% in the L1-7(N) group, 77% in the anti-VEGF antibody group, and 91% in the combination group (Fig. 1A, i). Tumor growth in the combination group was 76% less than in the L1-7(N) group and 61% less than in the anti-VEGF antibody group. At the end of 26 days of treatment, in comparison with the hFc controls, tumors weighed 36% less after L1-7(N), 44% less after anti-VEGF antibody, and 59% less after the inhibitor combination (Fig. 1A, ii).

Viable regions of tumors were identified by YO-PRO-1 staining of nuclei (Fig. 1B, i), which served as a fluorescent

Table 1. Taqman RT-PCR measurements of gene expression in tumors (mRNA copy number per 100 ng total RNA)

	Tumor type	mAng2	hAng2	mVEGF	hVEGF	mKDR	hKDR	mTie2	hTie2	Tumor age (d)	Mouse strain	*n* (mice)
1	Colo205	28,721	11,756	43,003	203,804	7,418	<1,000	<1,000	<1,000	23	CD1 *nu/nu*	5
2	HT29	21,165	4,560	160,551	822,448	5,877	<1,000	<1,000	<1,000	21	CD1 *nu/nu*	5
3	MCF-7	17,570	6,164	62,106	93,978	15,519	<1,000	<1,000	<1,000	36	CD1 *nu/nu*	4
4	CaPan1	15,412	5,027	166,781	275,542	4,672	<1,000	<1,000	<1,000	21	CD1 *nu/nu*	5
5	U87	15,024	17,878	15,209	945,551	10,831	1,429	<1,000	<1,000	24	CD1 *nu/nu*	5
6	ZR-75-1	12,816	10,272	22,526	208,325	23,244	<1,000	<1,000	<1,000	41	CD1 *nu/nu*	4
7	A431	11,463	4,006	47,087	1,876,894	9,786	<1,000	<1,000	<1,000	14	CD1 *nu/nu*	5
8	SKOV-3	11,293	267,957	105,024	738,549	19,358	1,895	<1,000	<1,000	57	CB17 SCID	5
9	DU 145	10,755	10,760	35,715	1,453,220	18,719	8,239	<1,000	<1,000	50	CD1 *nu/nu*	5
10	LN-229	9,729	7,239	65,982	392,494	6,787	1,842	<1,000	<1,000	19	CD1 *nu/nu*	5
11	Mes-Sa/Dx5	9,619	5,585	31,120	151,635	2,811	<1,000	<1,000	<1,000	23	CD1 *nu/nu*	5
12	H1299	9,171	4,822	59,130	107,959	13,357	<1,000	<1,000	<1,000	49	CD1 *nu/nu*	5
13	AsPC1	8,571	4,967	149,505	184,947	7,182	<1,000	<1,000	<1,000	21	CD1 *nu/nu*	5
14	BT-474	8,506	12,615	25,477	335,546	15,804	<1,000	<1,000	<1,000	30	CD1 *nu/nu*	4
15	PC-3	8,153	8,256	35,322	1,552,016	6,735	2,212	<1,000	<1,000	21	CD1 *nu/nu*	5
16	A673	6,954	6,799	70,615	240,016	22,835	<1,000	<1,000	<1,000	14	CD1 *nu/nu*	5
17	Raji	6,654	5,327	72,759	44,732	7,954	<1,000	<1,000	<1,000	22	CB17 SCID	5
18	HCT116	6,305	16,913	47,279	200,421	14,642	<1,000	<1,000	<1,000	20	CD1 *nu/nu*	5
19	SK-MES-PD	5,441	29,680	42,752	208,980	4,870	<1,000	<1,000	<1,000	13	CD1 *nu/nu*	5
20	Calu-6	5,200	35,734	79,808	42,350	9,697	<1,000	<1,000	<1,000	21	CD1 *nu/nu*	5
21	Colo320	4,051	7,681	20,629	207,112	3,040	<1,000	<1,000	<1,000	21	CD1 *nu/nu*	5
22	Daudi	3,713	22,571	18,791	105,753	1,821	<1,000	<1,000	<1,000	27	CD1 *nu/nu*	5
23	NAMALWA	3,384	13,167	19,671	83,868	5,050	<1,000	<1,000	<1,000	17	CB17 SCID	5
	Median	9,171	8,256	47,087	208,325	7,954						
	Mean	10,420	22,597	60,732	455,484	10,348						
	SE	1,258	11,286	9,396	109,789	1,335						
	n	23	23	23	23	23						

NOTE: Expression of human (h) and mouse (m) Ang2, Tie2, VEGF, and VEGFR-2 (KDR) in 23 human tumors implanted into immunocompromised CD1 nude or CB17 SCID mice for periods of 13 to 57 d (n = 4–5 mice per tumor type). Values shown as <1,000 were below level of detection by Taqman RT-PCR.

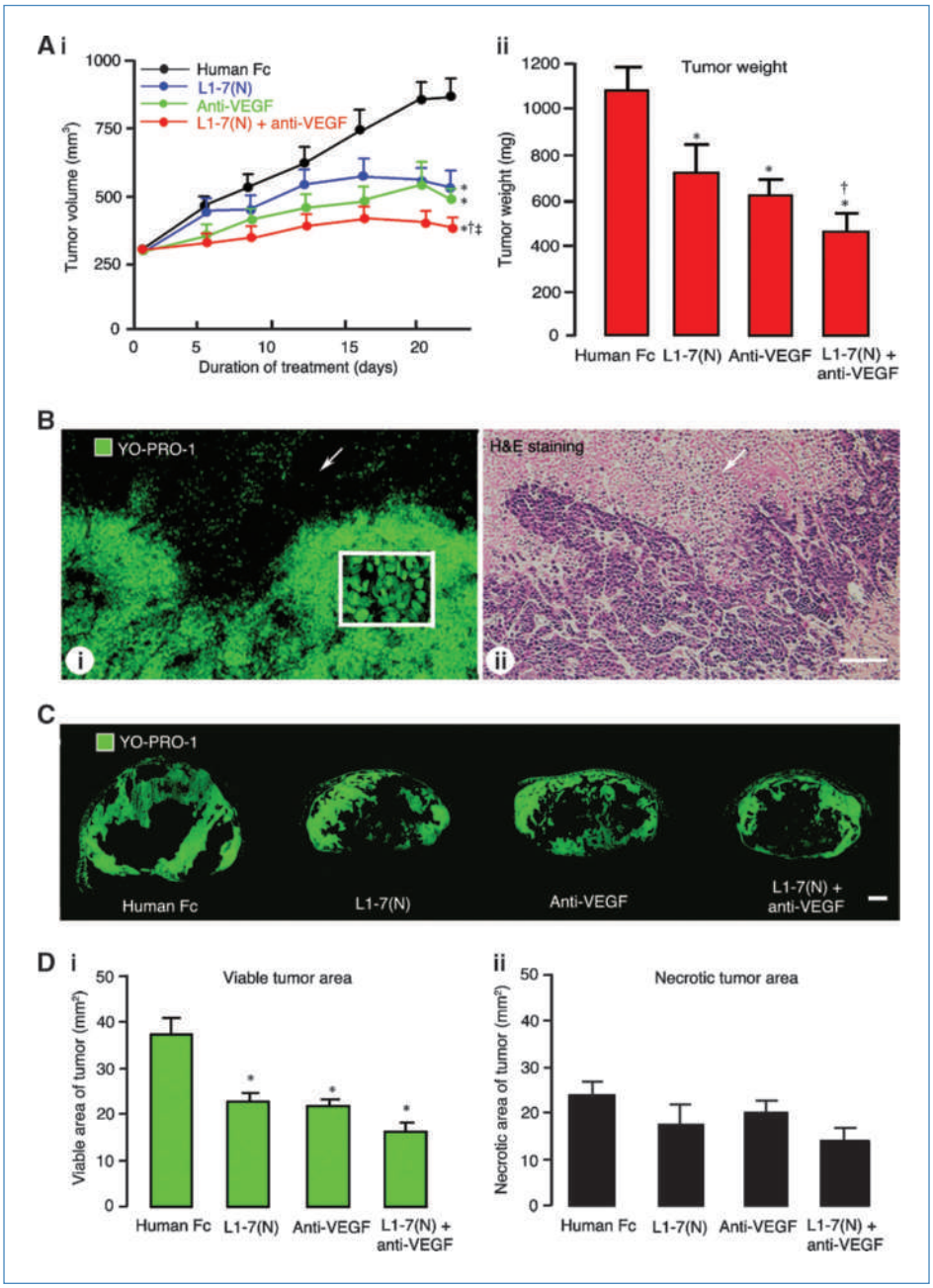

Figure 1. Changes of tumor growth, weight, and viable tumor cells after inhibition of Ang2, VEGF, or both. A, growth of Colo205 tumors treated with hFc, L1-7(N), anti-VEGF antibody, or the combination. i, L1-7(N) or anti-VEGF antibody slowed tumor growth and the combination slowed growth even more; ii, tumor weights after 26 d of treatment with hFc, L1-7(N), anti-VEGF antibody, or the combination. B, Colo205 tumor stained with YO-PRO-1 at day 7. i, viable tumor (bottom) is distinguishable from necrotic tumor (black, arrow) because of YO-PRO-1 staining of tumor cell nuclei (inset). ii, H&E-stained section of Colo205 tumor. Viable tumor with nuclei stained purple (bottom) is clearly distinguishable from diffusely pink stained necrotic regions (arrow). C, sections of Colo205 tumors at day 26 after treatment with hFc, L1-7(N), anti-VEGF antibody, or the combination. Compared with hFc treatment, viable tumor stained green with YO-PRO-1 was less after L1-7(N), anti-VEGF antibody, or the drug combination. D, size of viable tumor after 26 d of treatment. i, the amount of viable tumor was significantly smaller after treatment with L1-7(N), anti-VEGF antibody, or the combination; ii, tumor necrotic areas were not significantly different after 26 d of treatment. Scale bars, 150 μm (B, i), 100 μm (B, ii), and 1 mm (C). *, $P < 0.05$ versus hFc; †, $P < 0.05$ versus L1-7(N); ‡ $P < 0.05$ versus anti-VEGF.

equivalent to conventional staining by H&E (Fig. 1B, ii). Control tumors had large viable regions, but most also had large necrotic regions (Fig. 1C; Supplementary Fig. S1). After L1-7(N) or anti-VEGF antibody, the tumors were smaller in overall size and had smaller viable regions (Fig. 1C and D, i); however, the amount of necrosis was about the same as in control tumors (Fig. 1C and D, ii). Tumor cross-sectional area was even smaller after treatment with both inhibitors due largely to reduced viable tumor. Measurements revealed that the total area of viable tumor at day 26, relative to hFc-treated tumors, was 40% less after L1-7(N), 45% less after anti-VEGF antibody, and 55% less after the inhibitor combination (Fig. 1D, i).

After the dual inhibitors, the amount of necrotic tumor was slightly less in absolute amount but represented a larger proportion of the total tumor mass (Fig. 1D, i and ii). Necrosis tended to be greater near the center and less at the periphery in all groups of tumors (Supplementary Fig. S1). Central necrosis was particularly common after anti-VEGF antibody and the inhibitor combination but was also found in the other treatment groups (Supplementary Fig. S1).

Cell proliferation and apoptosis were assessed in viable regions of tumors stained for phosphohistone-H3 and activated caspase-3, respectively. Tumor cells were the predominant cell type in Colo205 tumors and were the predominant cell stained by markers of proliferation and apoptosis. At day 26, phosphohistone-H3–immunoreactive cells were abundant in tumors treated with hFc (Fig. 2A, i) but were less numerous after L1-7(N) (Fig. 2A, ii), anti-VEGF antibody (Fig. 2A, iii), or the inhibitor combination (Fig. 2A, iv). The area density of phosphohistone-H3 staining was significantly less after treatment with any of the active agents than after hFc, with reductions of 68% after L1-7(N), 63% after anti-VEGF antibody, and 67% after the inhibitor combination (Fig. 2B). Similarly, the total area of phosphohistone-H3 staining was 83% less after L1-7(N), 81% less after anti-VEGF antibody, and 82% less after the inhibitor combination (Fig. 2C).

Apoptotic cells identified by activated caspase-3 immunoreactivity were located throughout the viable regions of tumors in all groups treated for 26 days (Fig. 3A). Apoptotic cells tended to be more abundant after L1-7(N) (Fig. 3A, ii), anti-VEGF antibody (Fig. 3A, iii), or the inhibitor combination (Fig. 3A, iv). The amount of activated caspase-3 staining, expressed as a percentage of tumor area in comparison with the hFc control, doubled after L1-7(N) (Fig. 3B). The increase in apoptosis was not significant after the anti-VEGF antibody (48%) but was significant after the inhibitor combination (63%; Fig. 3B). The total area of staining expressed in absolute units (mm^2) was not significantly different among the four treatment groups (Fig. 3C), where increases in percentage of tumor stained were offset by decreases in tumor size.

Changes in tumor vascularity after treatment. Tumor blood vessels were examined to determine whether the decrease in proliferation and increase in apoptosis were attributable to vascular pruning. CD31-positive blood vessels in control tumors were abundant and tortuous, were uneven in size, and had numerous sprouts (Fig. 4A, i). Tumor vascular density was unchanged after treatment with L1-7(N) (Fig. 4A, ii), tended to be less after anti-VEGF antibody (Fig. 4A, iii), but was conspicuously reduced after treatment with the inhibitor combination (Fig. 4A, iv).

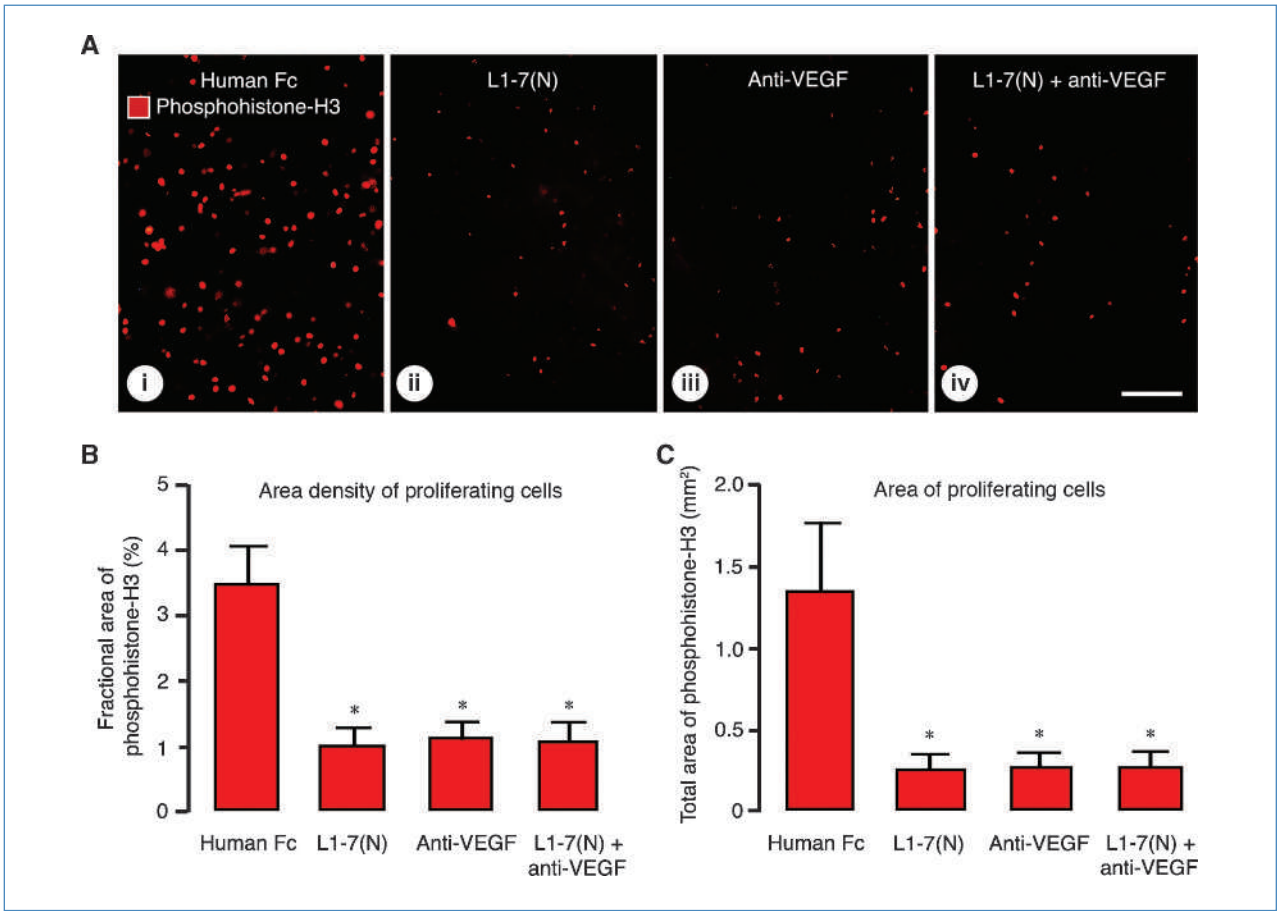

Figure 2. Treatment-related changes of tumor cell proliferation. A, phosphohistone-H3 immunoreactivity at day 26 of treatment with hFc (i), L1-7(N) (ii), anti-VEGF antibody (iii), or the combination (iv). Phosphohistone-H3–positive cells in viable regions were abundant after hFc but rare after L1-7(N), anti-VEGF antibody, or the combination. Scale bar, 150 μm. B and C, fractional area (area density; B) and total area (C) of proliferating tumor cells identified by phosphohistone-H3 immunoreactivity. Fractional area and total area were both significantly less at day 26 after L1-7(N), anti-VEGF antibody, or the combination than after hFc treatment (B and C). *, $P < 0.05$ versus hFc.

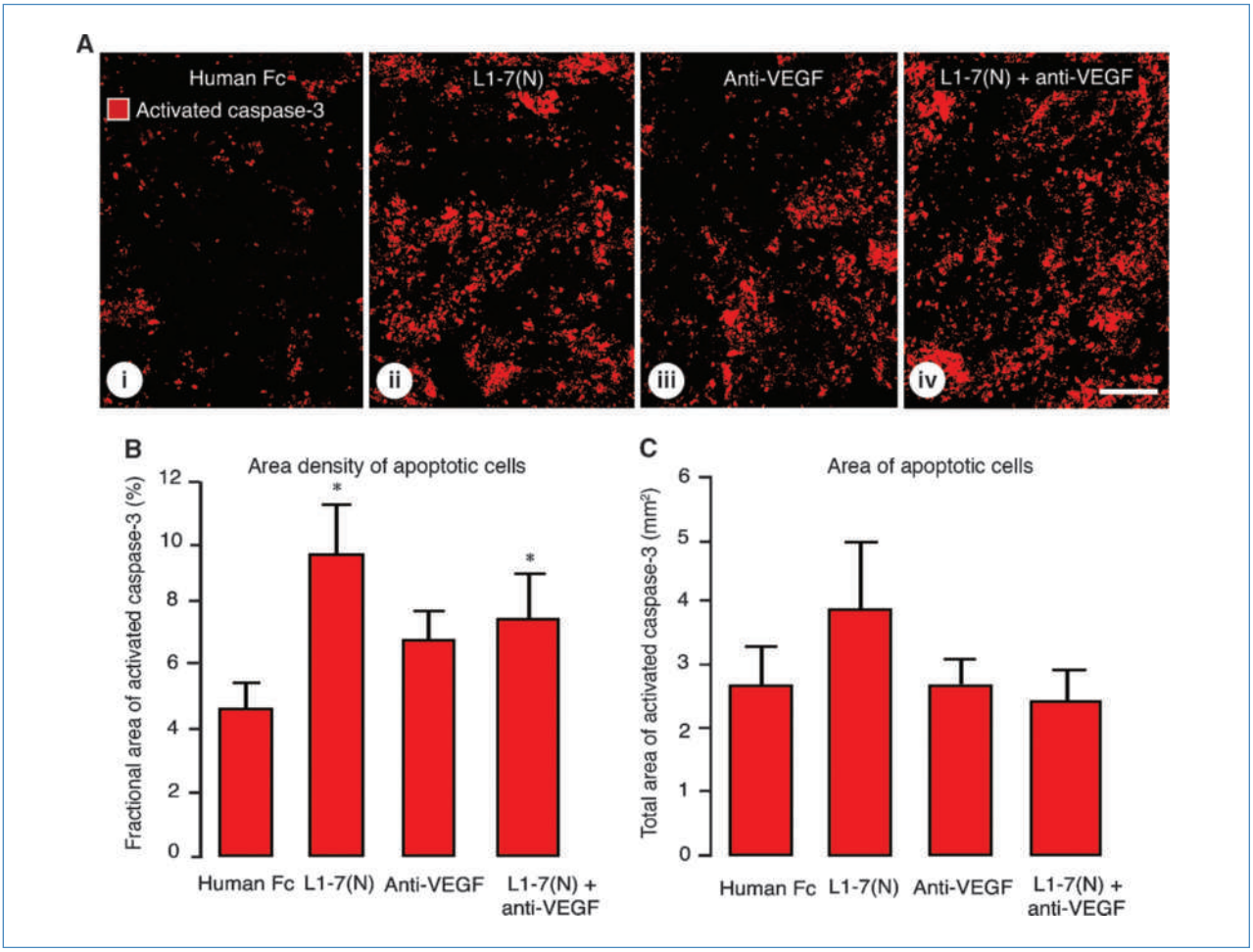

Figure 3. Treatment-related changes in tumor cell apoptosis. A, activated caspase-3 immunoreactivity after 26 d of hFc (i), L1-7(N) (ii), anti-VEGF antibody (iii), or the combination (iv). Activated caspase-3–positive tumor cells were abundant after L1-7(N) or the combination. Scale bar, 200 μm. B, fractional areas (area density) of apoptosis assessed by activated caspase-3 immunoreactivity at day 26. Area density of apoptotic cells was greater after L1-7(N) or the combination. C, total area of activated caspase-3–positive cells was not significantly different among the four treatment groups at day 26. *, $P < 0.05$ versus hFc.

Measurements confirmed that the fractional area (area density) of CD31 immunoreactivity did not change after L1-7(N), had a small but not significant reduction after anti-VEGF antibody, and had a large (67%) and significant reduction after the inhibitor combination (Fig. 4B). When the fractional area of tumor vessels was scaled for tumor size (values expressed in square millimeters of tumor) to take into account treatment-related differences in overall tumor size, the values were 37% less after L1-7(N), 51% less after anti-VEGF antibody, and 82% less after the combination of inhibitors for 26 days (Fig. 4C). Values for the inhibitor combination were 71% less than those after L1-7(N) alone (Fig. 4C). In addition to the effects on total tumor vessel area, blood vessels in tumors treated with L1-7(N) and anti-VEGF antibody, alone or in combination, were smoother, had fewer sprouts, and were smaller and more uniform in size (Fig. 4A).

Under baseline conditions, tumor vessels had sparse coverage by PDGFR-β–immunoreactive pericytes, but after L1-7(N) or anti-VEGF antibody, the vessels had a thick envelopment of pericytes (Fig. 4D). Pericyte coverage after the inhibitor combination was intermediate in amount (Fig. 4D, iv). Measurements of PDGFR-β–positive pericytes within 10 μm of the endothelium reflected the differences evident by confocal microscopy (Fig. 4D, v).

The presence of empty basement membrane sleeves, indicative of blood vessel regression (3), was examined by co-staining endothelial cells (CD31) and vascular basement membrane (type IV collagen) to determine whether the reductions in tumor vascularity were due to vessel regression or reduced angiogenesis. All treatment groups had scattered fragments of basement membrane (Fig. 5A, arrowheads), but empty basement membrane sleeves were more abundant after the anti-VEGF antibody or the inhibitor combination (Fig. 5A, iii and iv, arrows).

As an index of angiogenic activity, endothelial sprouts, identified as tapered endothelial processes that extended

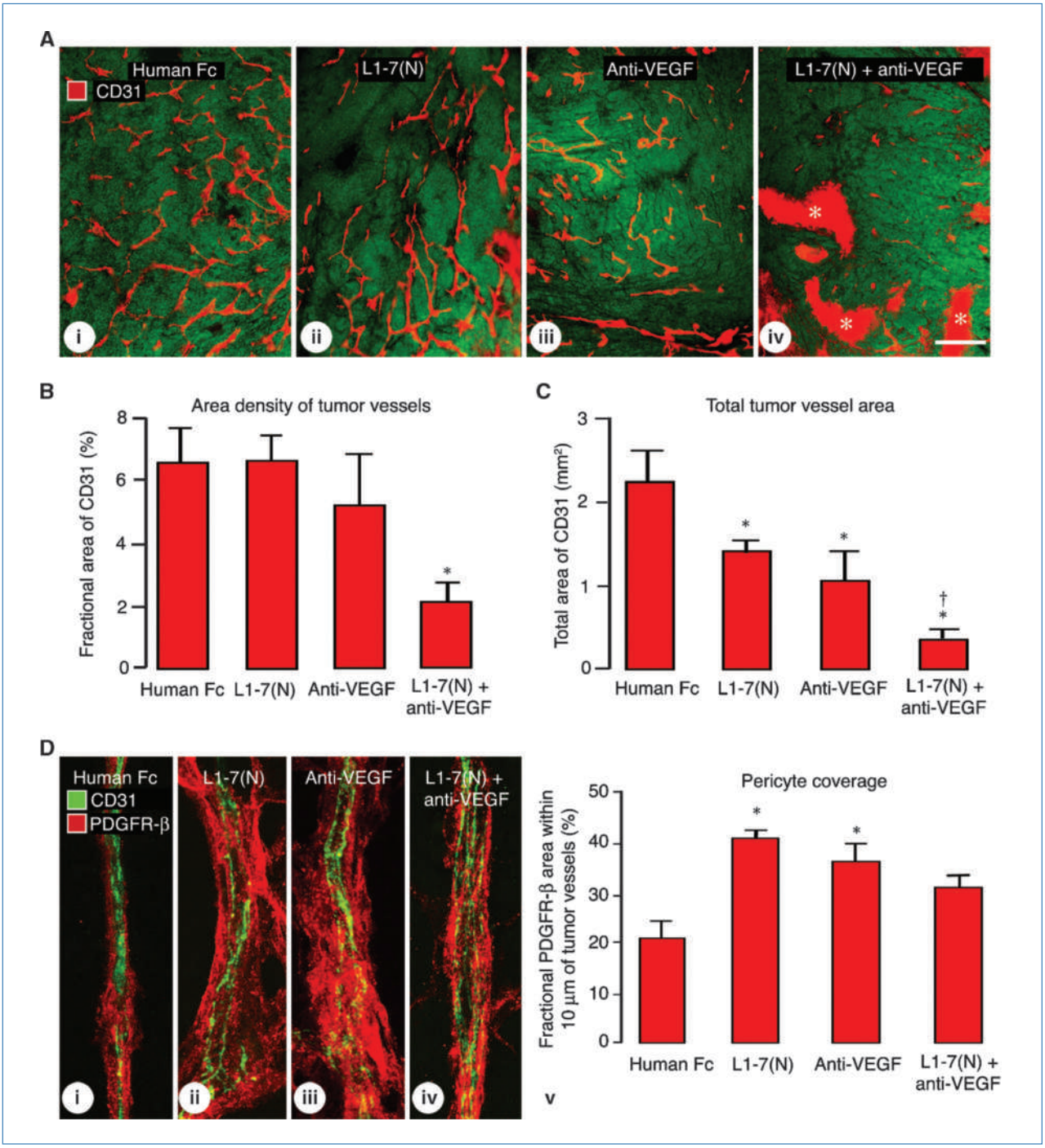

Figure 4. Treatment-related changes of tumor vascularity. A, fluorescent micrographs of CD31 immunoreactivity (red) in Colo205 tumors at day 26 after hFc (i), L1-7(N) (ii), anti-VEGF antibody (iii), or the combination (iv). The fractional area of CD31-positive blood vessels was less after the combination (iv) than after the other treatments (i–iii). Homogeneous red regions (asterisks in iv) indicate nonspecific staining of necrotic regions that were not included in measurements. Scale bar, 230 µm. B, fractional area of CD31 immunoreactivity in viable regions after 26 d of treatment with hFc, L1-7(N), anti-VEGF antibody, or the combination. At day 26, fractional vessel areas were less after the combination than after treatment with hFc or L1-7(N). C, total blood vessel area assessed by CD31 immunoreactivity in viable regions at day 26 after hFc, L1-7(N), anti-VEGF antibody, or the combination. At day 26, total vessel areas were less after L1-7(N), anti-VEGF antibody, and the combination than after hFc treatment. The total area after the combination was less than that after L1-7(N). D, confocal microscopic images of tumor vessels stained for CD31 (endothelial cells, green) and PDGFR-β (pericytes, red). i, some pericytes were associated with tumor vessels in controls (hFc). More pericytes were associated with tumor vessels after treatment with L1-7(N) (ii), anti-VEGF (iii), or the combination (iv). iv, area density of PDGFR-β staining within 10 µm of tumor vessels was significantly greater after L1-7(N) or anti-VEGF antibody alone for 26 d. Although the value tended to increase after the drug combination, the value did not reach statistical significance. *, $P < 0.05$ versus hFc; †, $P < 0.05$ versus L1-7(N).

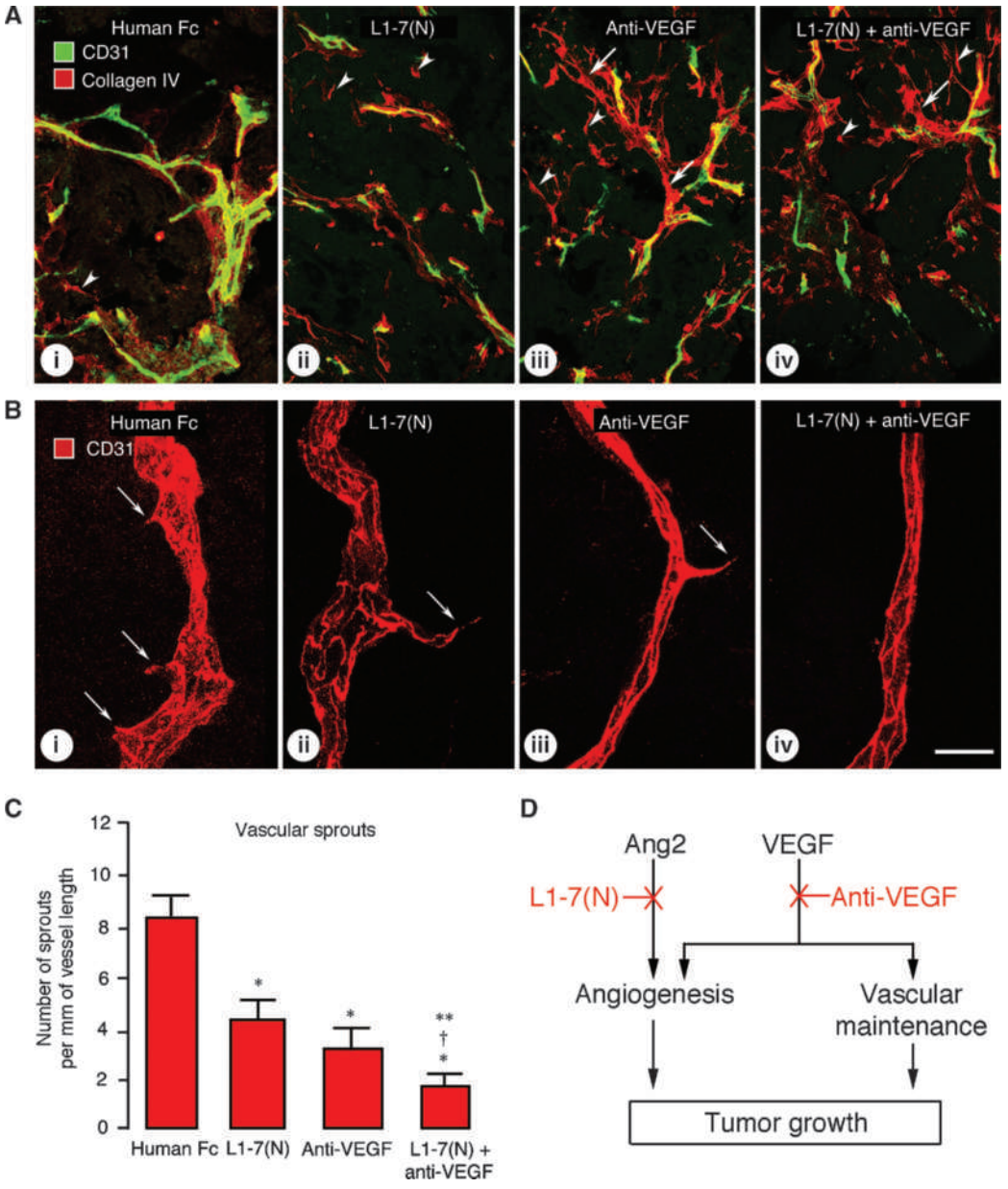

Figure 5. Empty basement membrane sleeves and endothelial sprouts. A, fragments of basement membrane (arrowheads, red) were visible in tumors from all treatment groups after staining for type IV collagen (red) and CD31-positive endothelial cells (green). Basement membrane sleeves that lacked endothelial cells were rare or absent in controls (i) or after L1-7(N) (ii) but were frequent after anti-VEGF antibody (iii) or the inhibitor combination for 26 d (iv). B, blood vessels had multiple sprouts (arrows) after hFc for 26 d (i) and fewer sprouts after L1-7(N) (ii), anti-VEGF antibody (iii), or the combination (iv). Scale bars, 150 μm (A) and 20 μm (B). C, number of sprouts per millimeter of blood vessel after hFc, L1-7(N), anti-VEGF antibody, or the combination for 26 d. After L1-7(N) and anti-VEGF antibody together, the density of sprouts was significantly less than after hFc. Sprouts were significantly less numerous after the combination than after hFc, L1-7(N), or anti-VEGF antibody. *, $P < 0.05$ versus hFc; †, $P < 0.05$ versus L1-7(N); **, $P < 0.05$ versus anti-VEGF antibody. D, diagram illustrating changes in Colo205 tumors after inhibition of Ang2 and/or VEGF. Inhibition of Ang2 by L1-7(N) reduced angiogenesis. Inhibition of tumor cell–derived VEGF with a function-blocking antibody reduced angiogenesis and also led to vascular regression. These reductions in tumor vessels were accompanied by reduced tumor growth. Inhibition of Ang2 and VEGF together led to greater reduction in tumor vascularity, angiogenesis, and growth.

from the main axis of vessels, were common on blood vessels of control tumors (Fig. 5B, i). Sprouts were less numerous after L1-7(N) or anti-VEGF antibody (Fig. 5B, ii and iii) and rare after the combination of inhibitors (Fig. 5B, iv). Measurements of the number of sprouts revealed reduction of 46% after L1-7(N), 62% after anti-VEGF antibody, and 82% after the inhibitor combination (Fig. 5C).

Discussion

This study sought to determine the effects on tumor cells and tumor blood vessels of the Ang2 inhibitor L1-7(N) and whether the changes complement the effects of inhibiting VEGF from tumor cells. Both the Ang2 and VEGF inhibitor decreased vessel sprouting and slowed tumor growth, but these changes were significantly greater when the two agents were combined than when either was given alone. The reduction in tumor growth was associated with decreased cell proliferation and increased apoptosis. Together, the results indicate that inhibition of Ang2 and VEGF together has additive effects on tumor growth and angiogenesis.

Effect of Ang2 and VEGF inhibition on tumor growth. Inhibition of Ang2 or VEGF slowed tumor growth, and inhibition of both together slowed tumor growth even more. The amount of necrosis did not change much with treatment, but slowing of tumor growth was accompanied by reduction in the amount of viable tumor, reduced cell proliferation, and increased apoptosis. Tumor cell apoptosis also increases after dual inhibition of Ang1 and Ang2 (13). Increased tumor cell apoptosis without a measurable increase in amount of necrosis may reflect more efficient clearance of cell debris, but further studies are needed to understand the fate of tumor cells that die.

After inhibition of Ang2, the fractional area of proliferating cells decreased and the fractional area of tumor cell apoptosis increased, but the total area occupied by apoptotic cells did not change significantly because the higher frequency of apoptotic events was offset by the reduction in tumor size.

Because YO-PRO-1 stains all nuclei, the values for tumor area reflect all cellular constituents. The identity of proliferating and apoptotic cells was not determined, but the predominance of tumor cells in Colo205 tumors makes it reasonable to assume that most phosphohistone-H3–positive or activated caspase-3–positive cells were tumor cells. Taken together, our findings suggest that most of the reduction in tumor growth resulted from a combination of decreased tumor cell proliferation and increased tumor cell apoptosis.

Inhibition of Ang2 and VEGF together had additive effects on decreasing tumor volume but not on proliferation, apoptosis, or necrosis. However, readouts for cell proliferation and death were only a snapshot of their effect at the end of the experiment. Changes in rate of cell proliferation or death occurring earlier in the 26-day experiment, well in advance of when the measurements were made, could have had disproportionate effects in slowing tumor growth.

Necrosis was present in tumors of all treatment groups and tended to be greatest centrally. Central necrosis, which was especially prominent after anti-VEGF antibody and the inhibitor combination, is a common feature of implanted xenografts that is usually attributed to higher interstitial pressure and poorer blood flow at the center of tumors (36, 37). Less necrosis at the perimeter may also reflect well-perfused vasculature of the surrounding normal tissue, although other properties that favor resistance of this region to inhibitors cannot be excluded.

Reduction of tumor vascularity and endothelial sprouting. The present findings are consistent with the familiar view that tumor growth is restricted by expansion of its blood supply and that reduced blood vessel growth will slow tumor growth proportionately. We found that the tumor vascularity was reduced after inhibition of Ang2 and VEGF together but was not significantly different among the other treatment groups. However, the total area of tumor blood vessels, scaled for tumor size, was reduced after Ang2 inhibition alone or after VEGF inhibition alone and was reduced even more when treatments were combined. These findings suggest that tumors grew synchronously with their blood vessels and maintained a constant ratio of blood vessels to tumor area, unless perturbed by inhibitors of both Ang2 and VEGF.

Angiogenesis inhibitors can reduce the number of tumor vessels by inhibition of endothelial sprouting and new vessel growth (35, 38) or by causing regression of existing vessels (3, 39). In this study, we sought to determine whether inhibition of Ang2 and VEGF together had additive effects on the reduction of tumor vascularity and growth. The present findings are consistent with previous results (31), showing that inhibition of Ang2 was followed by reduced endothelial sprouting without much regression of tumor vessels. Ang2 inhibition also increased the pericyte coverage of tumor vessels (31). These actions are consistent with the concept that Ang2 acts as a partial antagonist of Tie2 signaling, whereby Ang2 promotes vessel destabilization, unlike Ang1, which promotes vessel stabilization (14, 15). Together, these results indicate that Ang2 inhibition suppressed the growth of tumor vessels by blocking the destabilizing action of Ang2 on tumor vessels and unmasking the stabilizing action of Ang1.

In contrast, VEGF inhibition led to regression of tumor blood vessels and reduced endothelial sprouting, as found in previous studies (3, 40). Inhibition of VEGF and Ang2 together reduced the number of endothelial sprouts to an extent greater than either inhibitor alone. However, the appearance of empty basement membrane sleeves was evident only after the anti-VEGF antibody or the inhibitor combination. Thus, the greater reduction in tumor vessels after inhibition of VEGF and Ang2 together is likely to result from additive effects on endothelial sprout suppression and tumor vessel regression.

Benefits of targeting multiple antiangiogenic pathways. Recent studies suggest that targeting VEGF alone, although effective in eliminating some tumor blood vessels, only temporarily halts tumor growth and may even promote tumor aggressiveness and metastasis (40, 41). Anti-VEGF therapy is most effective when combined with chemotherapy or radiation (42). Another potentially beneficial strategy is to target multiple receptor tyrosine kinases in the hope of killing more tumor blood vessels than with anti-VEGF treatment alone. Multikinase inhibitors that target VEGF, PDGF, and other receptors were developed for this purpose and can eliminate more tumor blood vessels than anti-VEGF treatment alone (43–45). Inhibition of VEGF and PDGF together is more efficacious against all stages of pancreatic islet tumors in RIP-Tag2 mice than either inhibitor alone (46). The present findings indicate that a reasonable multitargeted approach

would be to combine inhibitors of Ang2 with inhibitors of VEGF signaling.

The downstream effects of angiogenesis inhibitors on tumor cells via blood vessels are incompletely understood, but these inhibitors can have complex effects on tumor growth (4, 34). Angiogenesis inhibitors are thought to slow tumor growth by eliminating blood vessels. VEGF inhibition reduces growth of some human cancers by stopping angiogenesis, destroying existing tumor vessels, and reducing blood flow (47, 48). Inhibition of PDGF-B can increase tumor growth in a preclinical model despite the regression of 80% of the blood vessels (34). Some angiogenesis inhibitors that clearly reduce tumor vascularity can paradoxically accelerate tumor invasiveness and growth (40, 41). Both the quantity and the quality of tumor vessels determine whether tumors grow or regress. The results of the present study revealed that tumor vascularity and tumor growth are tightly coupled in Colo205 tumors. Inhibition of Ang2 or VEGF alone led to decreased tumor vascularity and reduced tumor size, and the combination had complementary effects.

Other potential mechanisms for antitumor effects of Ang2 inhibition. By using species-specific probe sets, expression in tumors of human Ang2, Tie2, VEGF, and VEGFR-2/KDR in human Colo205 tumor cells could be measured separately from the corresponding mouse proteins in stromal cells. Measurements by Taqman RT-PCR revealed that expression of human tumor cell–derived VEGF was higher than mouse VEGF, but expression of mouse stromal cell–derived Ang2 and VEGFR-2 was higher than human. As there are far greater numbers of tumor cells than endothelial cells, these species differences in Ang2 and VEGFR-2 expression would be magnified if determined on a per-cell basis. These observations fit with published evidence for Ang2 expression in blood vessels of Colo205 tumors (13) and similar unpublished data for VEGFR-2 in these tumors. Tie2 expression was not detectable by quantitative RT-PCR or *in situ* hybridization, consistent with low expression or sparse distribution of Tie2 expression in endothelial cells, monocytes, or macrophages in Colo205 tumors. Together, these results are consistent with direct effects of Ang2 and VEGF inhibitors mainly on blood vessels in tumors. The reduction in tumor cell proliferation and increase in apoptosis are likely secondary to the vascular changes.

Inhibition of Ang2 may have additional beneficial effects in cancer therapy, which are mediated by mechanisms that are separate from the destabilizing effect of Ang2 on tumor vessels. Recent studies have reported that tumor-associated monocytes or macrophages express Tie2 receptors, can be recruited and/or activated by angiopoietins, and promote tumor angiogenesis by release of proteases that liberate sequestered VEGF from tumor matrix (49, 50). Further studies will be needed to determine whether inhibition of Ang2 signaling suppresses a macrophage-dependent mechanism that complements the direct effects of Ang2 inhibition on endothelial cells.

Possible mechanisms that explain the effects of inhibitors of Ang2 or VEGF, given alone or in combination, on tumor growth and angiogenesis are illustrated in Fig. 5D. Ang2 inhibition prevents the growth of new vessels by endothelial sprout formation. Reduced sprouting leads to less tumor cell proliferation, more tumor cell apoptosis, and smaller tumors. VEGF inhibition is followed by tumor vessel regression, the formation of empty basement membrane sleeves, and reduced tumor growth. Blockade of Ang2 and VEGF together has additive effects on sprouting and vessel regression and produces greater slowing of tumor growth. Together, our findings suggest that Ang2 inhibitors and VEGF inhibitors have complementary antiangiogenic actions and effects on reducing tumor growth.

Disclosure of Potential Conflicts of Interest

A. Coxon, D. Yu, J.V. Bready, and J.D. Oliner: employees and stockholders of Amgen, Inc. D.M. McDonald: commercial research grant, Amgen. The other authors disclosed no potential conflicts of interest.

Acknowledgments

We thank Jeyling Chou, Jennifer Feng, Talia Romano, Anne Saiki, and Ji-Rong Sun for technical assistance and Tatsuma Okazaki, Barbara Sennino, and Weon-Kyoo You for valuable discussions.

Grant Support

NIH/National Cancer Institute grant CA82923; NIH/National Heart, Lung, and Blood Institute grants HL24136, HL59157, and HL96511; Amgen; and AngelWorks Foundation (D.M. McDonald).

The costs of publication of this article were defrayed in part by the payment of page charges. This article must therefore be hereby marked *advertisement* in accordance with 18 U.S.C. Section 1734 solely to indicate this fact.

Received 05/30/2009; revised 12/09/2009; accepted 01/08/2010; published OnlineFirst 03/02/2010.

References

1. Ferrara N, Kerbel RS. Angiogenesis as a therapeutic target. Nature 2005;438:967–74.
2. Huang J, Frischer JS, Serur A, et al. Regression of established tumors and metastases by potent vascular endothelial growth factor blockade. Proc Natl Acad Sci U S A 2003;100:7785–90.
3. Inai T, Mancuso M, Hashizume H, et al. Inhibition of vascular endothelial growth factor (VEGF) signaling in cancer causes loss of endothelial fenestrations, regression of tumor vessels, and appearance of basement membrane ghosts. Am J Pathol 2004;165:35–52.
4. Jain RKTitle: Normalization of tumor vasculature: an emerging concept in antiangiogenic therapy. Science 2005;307:58–62.
5. Tong RT, Boucher Y, Kozin SV, Winkler F, Hicklin DJ, Jain RK. Vascular normalization by vascular endothelial growth factor receptor 2 blockade induces a pressure gradient across the vasculature and improves drug penetration in tumors. Cancer Res 2004;64:3731–6.
6. Borgstrom P, Gold DP, Hillan KJ, Ferrara N. Importance of VEGF for breast cancer angiogenesis *in vivo*: implications from intravital microscopy of combination treatments with an anti-VEGF neutralizing monoclonal antibody and doxorubicin. Anticancer Res 1999;19:4203–14.
7. Folkins C, Man S, Xu P, Shaked Y, Hicklin DJ, Kerbel RS. Anticancer therapies combining antiangiogenic and tumor cell cytotoxic effects reduce the tumor stem-like cell fraction in glioma xenograft tumors. Cancer Res 2007;67:3560–4.
8. Gerber HP, Ferrara N. The role of VEGF in normal and neoplastic hematopoiesis. J Mol Med 2003;81:20–31.
9. Fischer C, Jonckx B, Mazzone M, et al. Anti-PlGF inhibits growth of

VEGF(R)-inhibitor-resistant tumors without affecting healthy vessels. Cell 2007;131:463–75.
10. Blakey DC, Emery SC, Zhou Q, Kendrew J, Cao Z, Brown J. Identification of a human antibody 3.19.3 that inhibits ANG-2 function leading to significant anti-tumor activity in a panel of tumor xenograft models [abstract 137]. In: Proceedings of the 100th Annual Meeting of the American Association for Cancer Research; 2009 Apr 18-22; Denver, CO. Philadelphia (PA): AACR; 2009.
11. Herbst RS, Hong D, Chap L, et al. Safety, pharmacokinetics, and antitumor activity of AMG 386, a selective angiopoietin inhibitor, in adult patients with advanced solid tumors. J Clin Oncol 2009;27: 3557–65.
12. Hu B, Cheng SY. Angiopoietin-2: development of inhibitors for cancer therapy. Curr Oncol Rep 2009;11:111–6.
13. Oliner J, Min H, Leal J, et al. Suppression of angiogenesis and tumor growth by selective inhibition of angiopoietin-2. Cancer Cell 2004;6: 507–16.
14. Yancopoulos GD, Davis S, Gale NW, Rudge JS, Wiegand SJ, Holash J. Vascular-specific growth factors and blood vessel formation. Nature 2000;407:242–8.
15. Fiedler U, Augustin HG. Angiopoietins: a link between angiogenesis and inflammation. Trends Immunol 2006;27:552–8.
16. Holash J, Maisonpierre PC, Compton D, et al. Vessel cooption, regression, and growth in tumors mediated by angiopoietins and VEGF. Science 1999;284:1994–8.
17. Ahmad SA, Liu W, Jung YD, et al. The effects of angiopoietin-1 and -2 on tumor growth and angiogenesis in human colon cancer. Cancer Res 2001;61:1255–9.
18. Yu Q, Stamenkovic I. Angiopoietin-2 is implicated in the regulation of tumor angiogenesis. Am J Pathol 2001;158:563–70.
19. Lobov IB, Brooks PC, Lang RA. Angiopoietin-2 displays VEGF-dependent modulation of capillary structure and endothelial cell survival *in vivo*. Proc Natl Acad Sci U S A 2002;99:11205–10.
20. Zagzag D, Hooper A, Friedlander DR, et al. *In situ* expression of angiopoietins in astrocytomas identifies angiopoietin-2 as an early marker of tumor angiogenesis. Exp Neurol 1999;159:391–400.
21. Fukuhara S, Sako K, Minami T, et al. Differential function of Tie2 at cell-cell contacts and cell-substratum contacts regulated by angiopoietin-1. Nat Cell Biol 2008;10:513–26.
22. Saharinen P, Eklund L, Miettinen J, et al. Angiopoietins assemble distinct Tie2 signalling complexes in endothelial cell-cell and cell-matrix contacts. Nat Cell Biol 2008;10:527–37.
23. Zhang L, Yang N, Park JW, et al. Tumor-derived vascular endothelial growth factor up-regulates angiopoietin-2 in host endothelium and destabilizes host vasculature, supporting angiogenesis in ovarian cancer. Cancer Res 2003;63:3403–12.
24. Coxon A, Rex K, Sun J, et al. Combined treatment of angiopoietin and VEGF pathway antagonists enhances antitumor activity in preclinical models of colon carcinoma [abstract 1113]. In: Proceedings of the 99th Annual Meeting of the American Association for Cancer Research; 2008 Apr 12-16; San Diego, CA. Philadelphia (PA): AACR; 2008.
25. Hughes P, Polverino A, Oliner J, Kendall R. Angiopoietin-2 antagonists of anti-angiogenic therapy. In: Marme D, Fusenig N, editors. Tumor angiogenesis: basic mechanisms and cancer therapy. Berlin: Springer; 2007, p. 454–64.
26. Nasarre P, Thomas M, Kruse K, et al. Host-derived angiopoietin-2 affects early stages of tumor development and vessel maturation but is dispensable for later stages of tumor growth. Cancer Res 2009;69:1324–33.
27. Lin P, Buxton JA, Acheson A, et al. Antiangiogenic gene therapy targeting the endothelium-specific receptor tyrosine kinase Tie2. Proc Natl Acad Sci U S A 1998;95:8829–34.
28. Melani C, Stoppacciaro A, Foroni C, Felicetti F, Care A, Colombo MP. Angiopoietin decoy secreted at tumor site impairs tumor growth and metastases by inducing local inflammation and altering neoangiogenesis. Cancer Immunol Immunother 2004;53:600–8.
29. Sarraf-Yazdi S, Mi J, Moeller BJ, et al. Inhibition of *in vivo* tumor angiogenesis and growth via systemic delivery of an angiopoietin 2-specific RNA aptamer. J Surg Res 2007;146:16–23.
30. White RR, Shan S, Rusconi CP, et al. Inhibition of rat corneal angiogenesis by a nuclease-resistant RNA aptamer specific for angiopoietin-2. Proc Natl Acad Sci U S A 2003;100:5028–33.
31. Falcon BL, Hashizume H, Koumoutsakos P, et al. Contrasting actions of selective inhibitors of angiopoietin-1 and angiopoietin-2 on the normalization of tumor blood vessels. Am J Pathol 2009;175:2159–70.
32. Nelson DA, Tan TT, Rabson AB, Anderson D, Degenhardt K, White E. Hypoxia and defective apoptosis drive genomic instability and tumorigenesis. Genes Dev 2004;18:2095–107.
33. Rasband WS. Image J. Bethesda (MD): U.S. National Institutes of Health; 1997-2009, http://rsb.info.nih.gov/ig/.
34. Sennino B, Falcon BL, McCauley D, et al. Sequential loss of tumor vessel pericytes and endothelial cells after inhibition of platelet-derived growth factor B by selective aptamer AX102. Cancer Res 2007;67:7358–67.
35. Morikawa S, Baluk P, Kaidoh T, Haskell A, Jain RK, McDonald DM. Abnormalities in pericytes on blood vessels and endothelial sprouts in tumors. Am J Pathol 2002;160:985–1000.
36. Boucher Y, Baxter LT, Jain RK. Interstitial pressure gradients in tissue-isolated and subcutaneous tumors: implications for therapy. Cancer Res 1990;50:4478–84.
37. Wexler EJ, Gravallese EM, Czerniak PM, et al. Tumor biology: use of tiled images in conjunction with measurements of cellular proliferation and death in response to drug treatments. Clin Cancer Res 2000;6:3361–70.
38. Vajkoczy P, Farhadi M, Gaumann A, et al. Microtumor growth initiates angiogenic sprouting with simultaneous expression of VEGF, VEGF receptor-2, and angiopoietin-2. J Clin Invest 2002;109:777–85.
39. Baluk P, Falcon B, Hashizume H, Sennino B, McDonald DM. Cellular actions of angiogenesis inhibitors on blood vessels. In: Marme D, Fusenig N, editors. Tumor angiogenesis: basic mechanisms and cancer therapy. Berlin: Springer; 2007, p. 557–76.
40. Ebos JM, Lee CR, Cruz-Munoz W, Bjarnason GA, Christensen JG, Kerbel RS. Accelerated metastasis after short-term treatment with a potent inhibitor of tumor angiogenesis. Cancer Cell 2009;15:232–9.
41. Paez-Ribes M, Allen E, Hudock J, et al. Antiangiogenic therapy elicits malignant progression of tumors to increased local invasion and distant metastasis. Cancer Cell 2009;15:220–31.
42. Jain RK, Duda DG, Clark JW, Loeffler JS. Lessons from phase III clinical trials on anti-VEGF therapy for cancer. Nat Clin Pract Oncol 2006;3:24–40.
43. Erber R, Thurnher A, Katsen AD, et al. Combined inhibition of VEGF and PDGF signaling enforces tumor vessel regression by interfering with pericyte-mediated endothelial cell survival mechanisms. FASEB J 2004;18:338–40.
44. Motzer RJ, Michaelson MD, Redman BG, et al. Activity of SU11248, a multitargeted inhibitor of vascular endothelial growth factor receptor and platelet-derived growth factor receptor, in patients with metastatic renal cell carcinoma. J Clin Oncol 2006;24:16–24.
45. Polverino A, Coxon A, Starnes C, et al. AMG 706, an oral, multikinase inhibitor that selectively targets vascular endothelial growth factor, platelet-derived growth factor, and Kit receptors, potently inhibits angiogenesis and induces regression in tumor xenografts. Cancer Res 2006;66:8715–21.
46. Bergers G, Song S, Meyer-Morse N, Bergsland E, Hanahan D. Benefits of targeting both pericytes and endothelial cells in the tumor vasculature with kinase inhibitors. J Clin Invest 2003;111: 1287–95.
47. Sennino B, Raatschen H, Wendland M, et al. Correlative dynamic contrast MRI and microscopic assessment of tumor vascularity in RIP-Tag2 transgenic mice. Magnet Res Med 2009;62:616–25.
48. Willett CG, Boucher Y, di Tomaso E, et al. Direct evidence that the VEGF-specific antibody bevacizumab has antivascular effects in human rectal cancer. Nat Med 2004;10:145–7.
49. Du R, Lu KV, Petritsch C, et al. HIF1α induces the recruitment of bone marrow-derived vascular modulatory cells to regulate tumor angiogenesis and invasion. Cancer Cell 2008;13:206–20.
50. Venneri MA, De Palma M, Ponzoni M, et al. Identification of proangiogenic TIE2-expressing monocytes (TEMs) in human peripheral blood and cancer. Blood 2007;109:5276–85.